The Specific Recognition of a Cell Binding Sequence Derived from Type I Collagen by Hep3B and L929 Cells

Shih Tak Khew[†] and Yen Wah Tong*[,†,‡]

Department of Chemical & Biomolecular Engineering, and Division of Bioengineering, National University of Singapore, 21 Lower Kent Ridge Road, Singapore 119077

Received May 28, 2007; Revised Manuscript Received July 17, 2007

In this study, the affinity of two different cell types toward a specific cell binding sequence (Gly-Phe-Hyp-Gly-Glu-Arg or GFOGER) derived from type I collagen using peptide template (PT)-assembled collagen peptides of different triple helicity as a model for natural collagen is examined. A series of biophysical studies, including melting curve analysis and circular dichroism spectroscopy, demonstrated the presence of stable triple-helical conformation in the PT-assembled $(GPO)_3-GFOGER-(GPO)_3$, (GPO)−GFOGER−(GPO), and $(Pro\text{-}Hyp\text{-}Gly)_5$ solution. Conversely, non-templated peptides, except $(GPO)_3-GFOGER-(GPO)_3$, showed no evidence of assembly into triple-helical structure. Biological assays, including cell adhesion, competitive inhibition, and immunofluorescence staining, revealed a correlation of triple-helical conformation with the cellular recognition of GFOGER in an integrin-specific manner. The triple helix was shown to be important, but not crucial for cell adhesion to native collagen. Hep3B and L929 cells displayed significant differences in the recognition of GFOGER, mainly because of the differences in their expression of specific integrin receptors for collagen. For example, PT-assembled $(GPO)_3-GFOGER-(GPO)_3$ was shown to perform comparably to collagen for L929, but not Hep3B, cell adhesion. The result showed that a specific cell binding motif may not fully mimic the extracellular matrix (ECM) microenvironment, suggesting the need to use a combination of two or more cell binding sequences for targeting a wide range of integrin receptors expressed by a specific cell type to better mimic the ECM.

Introduction

Cell−extracellular matrix (ECM) interactions have been shown to control many cellular activities, including embryogenesis, homeostasis, and tissue remodeling and healing.[1,2] Cell adhesion is crucial for the assembly of individual cells into three-dimensional tissues, as most cells grown in vitro must adhere to a substrate to survive and proliferate.[3] It is known that cells in vivo adhere to the ECM, either directly to components of the collagen-rich interstitial matrix or to the basement membrane, which comprises a variety of adhesive proteins, including collagen, fibronectin, and laminin.[4] Therefore, in recent development of biomaterials, numerous cell binding sequences, such as Arg-Gly-Asp (RGD),[5,6] P-15,[7−10] and Gly-Phe-Hyp-Gly-Glu-Arg (GFOGER),[11,12] have been used to convey biofunctionality to these materials to engineer ECM-like bioadhesive surfaces. Among the ECMs, type I collagen can directly promote the adhesion and migration of numerous cell types, including hepatocytes, fibroblasts, melanoma, keratinocytes, and neural crest cells.[3,13−16] Several cell binding domains within the type I collagen macromolecules have also been identified and used as a biological substitute for animal-derived type I collagen.[11,17−21] However, little has been done to compare the specific recognition of different cell types to a specific collagen or ECM protein sequence.

Most cell integrin receptors interact in a conformation-independent manner with specific peptide sequences derived from ECM proteins, such as RGD[22−24] and YIGSR.[24−26] Conversely, the collagen integrin receptors, such as $\alpha_1\beta_1$, $\alpha_2\beta_1$, $\alpha_3\beta_1$, $\alpha_{10}\beta_1$, and $\alpha_{11}\beta_1$,[27−32] bind to several regions within the triple-helical domain of collagen in a conformation-dependent manner.[18,21,33−35] Both conformation-dependent and conformation-independent sites may coexist within type I collagen.[19,27] Recent studies have revealed that GFOGER hexapeptide derived from residues 502−507 of collagen α1 (I) is a major cell binding site within type I collagen.[21,33] To understand the recognition of different cell integrin receptors to this specific cell binding sequence (GFOGER) and the structural basis of the recognition, a series of collagen-like peptides of different triple-helix stabilities were synthesized in this study. The integrin-specific GFOGER sequence was incorporated into the collagen peptides not only to promote cell adhesion but also to study its specific recognition by different cell types. A peptide template (PT) composed of Gly-Phe-Gly-Glu-Glu-Gly (GFGEEG) hexapeptide, characterized by its unique collagen-like primary structure and repeating Xxx-Yyy-Gly sequences, was used to assemble short collagen peptides into a triple-helical conformation that resembles the native structure of collagen (Figure 1).

This work focuses on using peptide−template assembled collagen peptides to promote mammalian cell adhesion and studying the recognition of two different cell types, namely, Hep3B and L929 cells, to a specific cell binding sequence (GFOGER) derived from type I collagen and the structural basis of the recognition. The conformational characterization of the collagen peptides was accomplished using circular dichroism (CD) spectroscopy, Rpn value comparison, and melting curve analysis. The cell binding activity was studied through a series of biological assays, including cell adhesion, cell competition inhibition, and cytoskeletal organization and focal adhesion immunofluorescence staining. This study may provide a better understanding of the specific recognition of a cell binding sequence by different cell types and the need to use specific

* Corresponding author. E-mail: chetyw@nus.edu.sg. Tel: (+65) 6516-8467. Fax: (+65) 6779-1936.
[†] Department of Chemical & Biomolecular Engineering.
[‡] Division of Bioengineering.

10.1021/bm700587j CCC: $37.00
Published on Web 09/14/2007

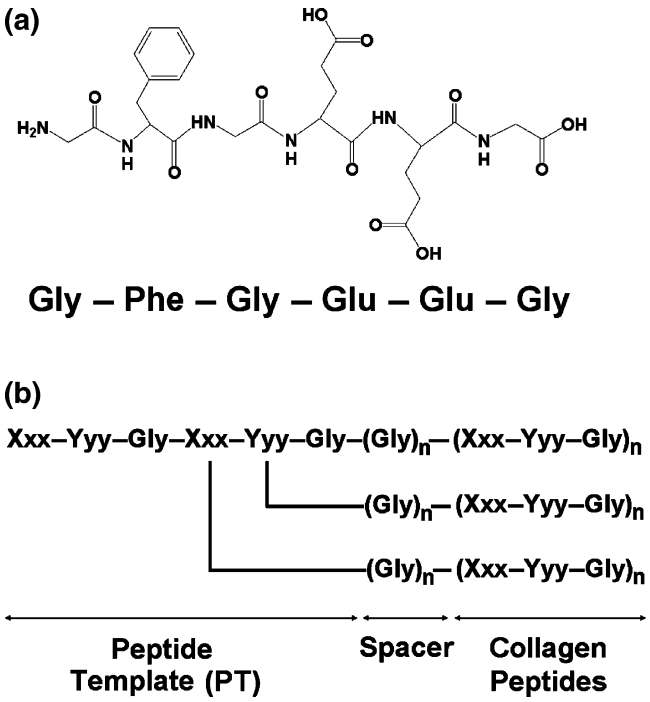

Figure 1. (a) Molecular structure of the GFGEEG PT. The C-terminal of the template contains three carboxyl groups, each of which can be linked to a strand of collagen peptide to facilitate the interactions of the three peptide chains to form the triple-helical conformation. (b) The PT-assembled collagen peptides. The template has a primary structure of repeating Xxx-Yyy-Gly triplets that is similar to that of collagen.

cell binding sequences for precisely controlling adhesion of a particular cell type.

Experimental Section

Materials. All peptide synthesis chemicals and solvents were of analytic reagent grade or better, and were purchased from Novabiochem except where noted. All amino acids were of l-configuration and purchased from Novabiochem. All chemicals were purchased from Sigma-Aldrich unless otherwise stated. Acetonitrile (high-performance liquid chromatography (HPLC) grade) was purchased from Merck.

Peptide Synthesis. The PT-assembled collagen peptides (PT-CP1, PT-CP2, and PT-CP3) as shown in Table 1 were synthesized using the fluorenyl-methoxy-carbonyl (Fmoc)−solid-phase peptide synthesis method. The N- and C- termini of all peptides were left as free amine and carboxylic acid, respectively. Fmoc−GFGEEG hexapeptide was first synthesized on the resin (50 μmol based on the resin substitution level). Stepwise couplings of amino acids were accomplished using a double coupling method with 5-fold excesses of amino acids, equivalent activator reagents 2-(1H-benzotriazole-1-yl)-1,1,3,3-tetramethyluronium hexafluorophosphate (HBTU) (Advanced Chemtech) and *N*-hydroxy-benzotriazole (HOBt) (Advanced Chemtech), and two equivalents of the base *N*-methylmorpholine (NMM). Each coupling reaction was allowed to proceed for 0.5 h at room temperature. All Fmoc-protected amino acids and activators were dissolved in dimethylformamide (DMF), except where noted, to saturation. Fmoc−Phe was dissolved in 1-methyl-2-pyrrolidone (NMP). The saturation concentration of Fmoc−amino acids in DMF or NMP is 0.6 M, while the saturation concentrations of HBTU and HOBt in DMF are 0.6 and 2.2 M, respectively. NMM was prepared in DMF at 45% (v/v) concentration. The removal of Fmoc was accomplished by using 20% (v/v) piperidine in DMF for 15 min twice. The resin was washed four times with DMF. Cycles of deprotection, washing, double couplings, and washing were repeated until the desired sequence was achieved. The Fmoc protection group at the N-terminal of the peptide was not removed. The product was washed with dichloromethane (DCM) twice and vacuum-dried prior to cleavage from resin using a cocktail solution composed of 95% trifluoroacetic acid, 2.5% deionized water, and 2.5% triisopropylsilane (v/v). The reaction was allowed to proceed for 3 h with occasional shaking. The cleavage solution was added to cold methyl *tert*-butyl ether dropwise to induce precipitation of the peptide. The precipitate was collected by centrifugation and was washed three times with an excess of cold ether to remove any residual scavengers. The final precipitate was redissolved and lyophilized.

Table 1. Melting Point Temperature (T_m) of the PT-Assembled Collagen Peptides and Their Nontemplated Counterparts as Determined by Temperature-Dependent UV Absorbance Measurement at 225 nm[a]

protein/peptides	sequence[b]	T_m (°C)
PT-CP1	(GFGEEG)≡ [G-(POG)$_5$]$_3$	61
PT-CP2	(GFGEEG)≡ [GG-GPO**GFOGER**GPO-GG]$_3$	20
PT-CP3	(GFGEEG)≡ [G-(GPO)$_3$**GFOGER**(GPO)$_3$-G]$_3$	44
CP1	(POG)$_5$	no transition
CP2	GPO**GFOGER**GPO	no transition
CP3	(GPO)$_3$**GFOGER**(GPO)$_3$	25
(Pro-Pro-Gly)$_3$	(PPG)$_3$	no transition
(Pro-Hyp-Gly)$_{10}$	(POG)$_{10}$	60
collagen	calf-skin collagen	37

[a] Cell recognition site (GFOGER) corresponding to residues 502−507 of the collagen α1 (I) is shown in bold. Each GFGEEG PT contains three carboxylic arms at its C-terminal for covalent coupling to the N-terminal of the collagen peptides. [b] Standard one-letter code is used to express amino acid sequences, except where noted. O represents hydroxyproline residue.

The collagen peptides (CP1, CP2, and CP3) were synthesized as described above, except that the Fmoc protection group at the N-terminal of the peptide was removed using 20% piperidine. Fmoc−GFGEEG (8 μmol) was dissolved in DMF to saturation (0.3 M) and added to the reaction vessel together with an equivalent of HBTU and HOBt, and 2 equiv of NMM, with respect to the carboxylic arms on the PT. The coupling of the PT to the N-termini of the collagen peptides proceeded for 6 h at room temperature with occasional shaking. The Fmoc protection group was removed as described above. The resin was washed with DMF and DCM twice and vacuum-dried overnight. The cleavage was done as described above. Preparative HPLC was performed to give products of purity greater than 85%, as given by the analytical HPLC. The molecular weight of the peptides was examined using matrix assisted laser desorption ionization time-of-flight mass spectrometry (MALDI-TOF MS).

CD Spectroscopy. CD measurements were performed on a Jasco model J-810 spectropolarimeter (Jasco, UK) using a quartz cylindrical cuvette (Hellma, Germany) with a path length of 0.1 mm to obtain mean residue molar ellipticity for each sample. The cuvette was filled with 150 μL of samples for each measurement. The CD spectra were obtained by continuous wavelength scans (average of three scans) from 260 to 180 nm at a scan speed of 50 nm/min. All samples were dissolved in ultrapure water, unless otherwise stated, and stored at 4 °C for at least 7 days prior to the test to allow for proper equilibration of triple-helical conformation. The samples were equilibrated for at least an hour at the desired temperature before the CD spectrum was acquired. PT-CP1, CP1, (POG)$_{10}$, and (PPG)$_{10}$ are generally neutral in water of pH 6−7, while PT-CP2, PT-CP3, CP2, and CP3, and the calf-skin collagen are more acidic in water of pH 3−4.

Melting Studies. The temperature-dependent UV absorbance of the peptides was measured on a Cary 50 Bio UV spectrophotometer (Varian,) equipped with a Peltier temperature controller (Quantum Northwest,).[36,37] Prior to any measurements, all samples were equilibrated at the initial temperature for at least 24 h. The samples were allowed to equilibrate at least 15 min until the UV absorbance was

time-independent at each subsequent temperature point. Data were collected at 225 nm.

Cell Culture. Hep3B liver cells and L929 fibroblast cells (ATCC) were cultured separately in Dulbecco's modified Eagle's medium (DMEM) (Gibco) supplemented with 10% fetal bovine serum (Hyclon), 110 mg/L sodium pyruvate (Sigma-Aldrich), 1% antimycotic solution (Sigma-Aldrich), and 1% nonessential amino acids (Sigma). The cells were maintained in a 75 cm^2 T-flask and incubated at 37 °C in the presence of 5% CO_2 and 95% relative humidity in an Autoflow NU-4850 CO_2 water-jacketed incubator (NuAire, Inc.).

Cell Adhesion Assay. Nunclon Delta TC 96-well plates were coated with 100 μL of 50 μg/mL collagen peptides or calf-skin collagen solution at 4 °C overnight, blocked with 100 μL of 1% heat-denatured bovine serum albumin (BSA) (Sigma-Aldrich), and then washed with phosphate buffered saline (PBS) two times. Denatured collagen peptides and collagen substrates were prepared in a similar way, except that the samples were first heated to 70 °C for 3 h immediately before incubation in the microwell plate at 70 °C overnight.[3] A 100 μL portion of the cell suspension in serum-free DMEM (10×10^5 cells/mL) was then added and incubated for 1 h at room temperature (20 °C). The plates were washed with PBS two times to remove the unattached cells. Adhered cells were measured by a total DNA quantification assay Hoechst 33258 (Sigma-Aldrich). Briefly, the cells were lysed by freeze−thaw cycles thrice in ultrapure water, and the cell lysates were mixed with 2 μg/mL bisbenzimide in 10 mM Tris-HCl (pH 7.4), 1 mM EDTA, and 0.2 M NaCl fluorescence assay buffer and were incubated in the dark for 30 min. The fluorescence was quantified on a microplate reader using 360 nm as the excitation and 465 nm as the emission wavelength. For all substrates, $n = 6$, and the data were expressed as mean ± standard deviation (SD).

Competition Inhibition Assay. Plates were coated with 100 μL of 50 μg/mL calf-skin collagen solution as described above. Cells (10×10^5 cells/mL) were incubated with 50 μg/mL peptides or collagen in serum-free DMEM to saturate the cell surface receptors for 30 min before seeding. For each competition assay, 100 μL of the cell suspension was seeded to the collagen-coated well, and the competitive adhesion was allowed to take place for 1 h at room temperature (20 °C). The assay was undertaken in triplicate, and the data were presented as mean ± SD. The attached cells were measured by the total DNA quantification method as described above. The adhesion of cells in the blank serum-free medium was used as a 100% reference level.

Immunofluorescence Staining for Actin Organization and Focal Adhesions. Substrate preparation was done as described above on a Lab-Tek chambered coverglass. Cells were seeded at a density of 280 cells/mm^2 in serum-free medium for 3 h. Attached cells were fixed in cold 3.7% formaldehyde for 5 min, permeabilized in 0.1% Triton X-100 for 5 min, and blocked in blocking buffer (1% BSA in PBS) for 0.5 h. Direct immunofluorescence staining of the cells with monoclonal antivinculin fluorescein isothiocyanate (FITC) conjugate (1:100 dilution in PBS) was allowed to proceed for 1 h. Staining for the actin cytoskeleton and cell nucleus was done by incubating the cells with phalloidin−tetramethylrhodamine isothiocyanate (TRITC) (1:1000 dilution in PBS) for 1 h and with 4′,6-diamidino-2-phenylindole (DAPI) (1:1000 dilution in PBS) for 5 min. A Zeiss LSM510 META confocal microscope (Zeiss, Germany) was used for imaging.

Statistical Analysis. The data of cell adhesion and competition inhibition are presented as mean ± SD. The statistical analysis of the data was done using Student's *t* test. A 95% confidence level was considered significant.

Results and Discussion

Structural Characterization by CD Spectroscopy, Rpn Value Comparison, and Melting Curve Analyses. The PT-assembled collagen peptides are distinguished from other protein and collagen mimetics[38−47] by the introduction of a PT, characterized by its collagen-like primary structure, and its completely amino acid-based contents, consistent with the native protein. On the basis of the mass of the peptides obtained after HPLC purification, the yields of the PT-assembled CP1, CP2, and CP3 were approximately 2%, 9%, and 1.7%, respectively. MALDI-TOF MS was used to verify the identity of each product, and the result (see Figures S1, S2, and S3 in the Supporting Information) showed that the molecular weight of each product obtained is consistent with that of the desired product: PT-CP1 $[M + H]^+ = 4776.4$ (calculated = 4776.5), $[M + Na]^+ = 4799.39$ (calculated = 4799.5); PT-CP2 $[M + H]^+ = 4864.1$ (calculated = 4864.04), $[M + Na]^+ = 4887.1$ (calculated = 4887.04); and PT-CP3 $[M + H]^+ = 7729.55$ (calculated = 7729.4), $[M + Na]^+ = 7752.43$ (calculated = 7752.4).

The conformation of the collagen peptides was characterized using CD spectroscopy. Natural collagen exhibits a unique CD spectrum characterized by a positive peak at around 220 nm, a crossover near 213 nm, and a large negative peak at approximately 197 nm.[48,49] Non-templated $(Pro\text{-}Hyp\text{-}Gly)_{10}$ was used as a stable prototype of a triple helix, while $(Pro{-}Pro\text{-}Gly)_3$ and calf-skin collagen were used as a negative control and collagen model, respectively. The PT-assembled collagen peptides and CP3 exhibited CD spectra features characteristic of a collagen-like triple helix, including a positive peak around 220−225 nm and a large negative trough near 200 nm (Figure 2), similar to natural collagen and $(Pro\text{-}Hyp\text{-}Gly)_{10}$ (Figure 2d). The establishment of triple-helical conformations by CD spectral band positions was also supported by comparing the CD spectra of the PT-assembled collagen peptides with that of native collagen after thermal denaturation. At elevated temperature (a significant decrease in the intensity of both positive and negative peaks of calf-skin collagen was observed) resulted in a CD spectrum similar to that of $(Pro{-}Pro\text{-}Gly)_3$ (result not shown), indicating a thermal transition from the folded to unfolded state. A similar trend was observed for the CD spectra of the PT-assembled collagen peptides at higher temperatures (Figure 2). However, the degree of conformational change is much smaller, probably because of the stabilizing effect of the template, which promotes interactions between the peptides and overcomes the unfavorable entropy. Conversely, the nontemplated CP1 and CP2 displayed CD spectra (Figure 2) characteristic of a polyproline II-like structure, as can be seen from the shallow peak at around 200 nm and the lack of the positive peak.[41,50] The patterns of these CD spectra are similar to that of a $(Pro{-}Pro\text{-}Gly)_3$ single-chain peptide, as given in Figure 2d, which is known to have no triple-helical conformation in solution.

Rpn values denote the ratio of positive and negative peak intensities in the CD spectra.[36,41] The CD spectra absorbance and Rpn values of the PT-assembled collagen peptides, listed in Table S1 (Supporting Information), are comparable to that of calf-skin collagen. Higher Rpn values were obtained for PT-CP1 (0.10), PT-CP2 (0.14), PT-CP3 (0.17), and CP3 (0.09) as compared to the nontemplated CP1 and CP2, which have Rpn values ranging from 0.03 to 0.04. The PT-assembled collagen peptides and CP3 have Rpn values close to or higher than that of collagen (0.12) and $(Pro\text{-}Hyp\text{-}Gly)_{10}$ (0.10). These results suggest that the PT-assembled collagen peptides and CP3 are triple-helical, while the nontemplated CP1 and CP2 are not.

Triple helices melt in a highly cooperative manner as the structures are stabilized by both intra- and interstrand hydrogen-bonding water networks[51−53] and thus can be distinguished from the polyproline II-like and nonsupercoiled structures on the basis of their thermal melting characteristics.[51] The melting transition

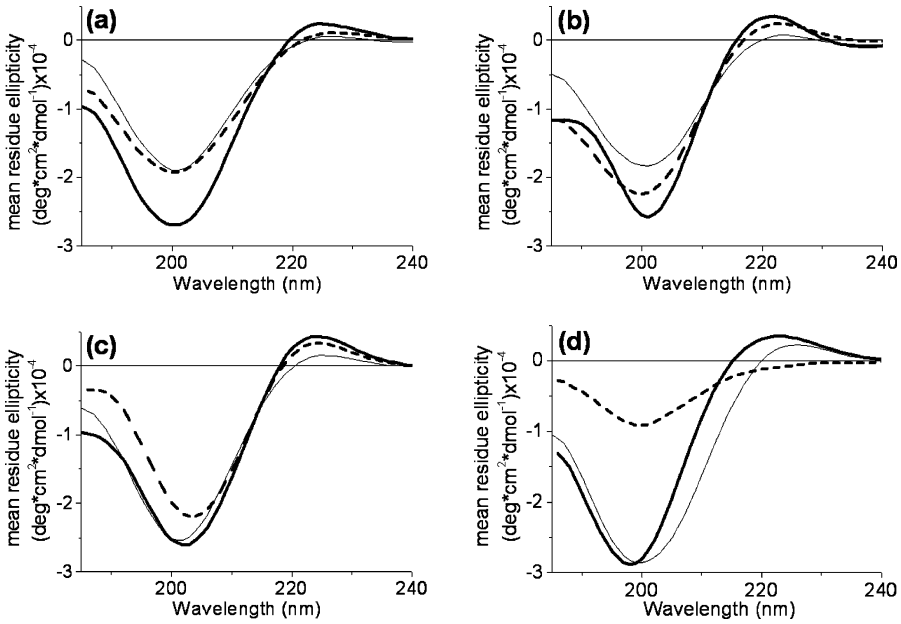

Figure 2. CD spectra of nontemplated (solid thin line), PT-assembled (solid thick line), and thermally denatured PT-assembled (dashed line) (a) $(POG)_5$, (b) (GPO)−GFOGER−(GPO), and (c) $(GPO)_3$-GFOGER-$(GPO)_3$. (d) CD spectra of collagen (solid thick line), $(POG)_{10}$ (solid thin line), and $(PPG)_3$ (dashed line). Samples were at 0.50 mg/mL in water.

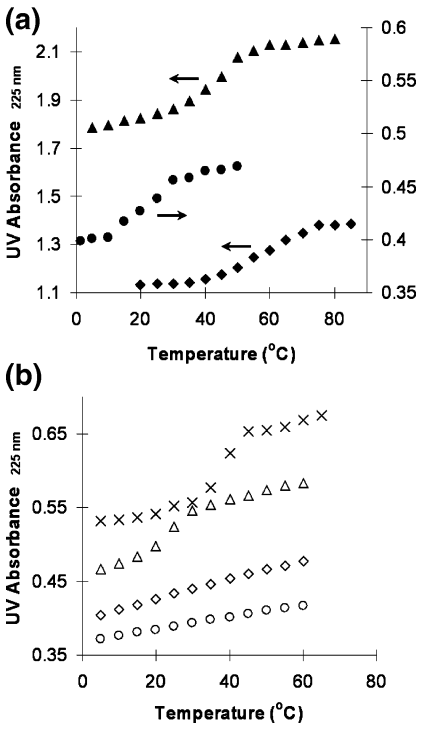

Figure 3. Melting transition curves of (a) PT-assembled collagen peptides: PT-CP1 (0.50 mg/mL) (◆), PT-CP2 (0.50 mg/mL) (●), and PT-CP3 (0.50 mg/mL) (▲), and (b) calf-skin collagen (0.50 mg/mL) (×) and non-templated collagen peptides: CP1 (0.55 mg/mL) (◇), CP2 (0.50 mg/mL) (○), and CP3 (0.70 mg/mL) (△).

curves are given in Figure 3. The midpoint of the transition was taken as the melting point temperature (T_m) and is presented in Table 1. It can be seen from Figure 3b that the nontemplated CP1 and CP2 showed curves with no transition and thus no evidence of triple helicity, even at low temperatures. The R^2 values for these curves obtained by a linear fitting are greater than 0.995, suggesting that these melting curves are a linear line with no transition. The use of the PT in promoting the assembly of short peptide sequences into triple-helical conformations is clearly seen by the cooperative melting curves displayed by PT-CP1, PT-CP2, and PT-CP3 as given in Figure 3a, similar to that of the native collagen (Figure 3b). While non-templated $(Pro\text{-}Hyp\text{-}Gly)_5$ showed no transition, PT-CP1 composed of three short $(Pro\text{-}Hyp\text{-}Gly)_5$ peptides exhibited a cooperative melting curve in water with a T_m of 58 °C. The melting temperature of $(Pro\text{-}Hyp\text{-}Gly)_{10}$ in water is 60 °C (result not shown), which is quite close to the T_m of PT-CP1. Therefore, it can be seen that the stabilizing effect of the PT is similar and equivalent to the addition of five more Pro-Hyp-Gly repeats to the nontemplated $(Pro\text{-}Hyp\text{-}Gly)_5$ chain. The result proves the significant role of the PT in the assembly of short collagen peptide chains into stable triple helices in solution. PT-CP2 and PT-CP3 supplemented with an integrin-specific GFOGER sequence[21,33] were also found to have stable triple-helical conformation with $T_m \approx 20$ and 40 °C, respectively. The observation of a cooperative transition curve together with a proper CD spectrum is indicative of the presence of stable triple-helical conformation.[54] It is clear that substitution of the cell binding domain into Pro-Hyp-Gly repeats may destabilize the triple helix, as seen from the lower T_m. However, the co-oligomeric structures are still able to form triple helices.

Hep3B Liver and L929 Fibroblast Cell Adhesion on PT-Assembled and Nontemplated Collagen Peptides. A cell adhesion assay was performed to study the recognition of Hep3B liver cells and L929 fibroblast cells for a specific cell binding sequence (GFOGER) derived from residues 502−507 of collagen α_1(I). The cell adhesion result is presented in Figure 4. Collagen and heat-denatured BSA were used as a positive and negative control in this assay, respectively. Cell adhesion to collagen was used as the 100% reference level.

It can be seen from Figure 4 that the maximum adhesion of both Hep3B (~60%) and L929 (~90%) cells occurred on the PT-CP3 surface. PT-CP2 and CP3 supported cell adhesion at a comparable level. The presence of both PT-CP2 and CP3 promoted modest but significant adhesion of Hep3B (average ~40%) and L929 (average ~73%) cells. The cell adhesion to GFOGER appeared to be conformation-dependent, as can be observed from the cell adhesion level on PT-CP3, PT-CP2, CP3, and CP2. Biophysical studies demonstrated that PT-CP3 adopts stable triple-helical conformation, while PT-CP2 and CP3 have

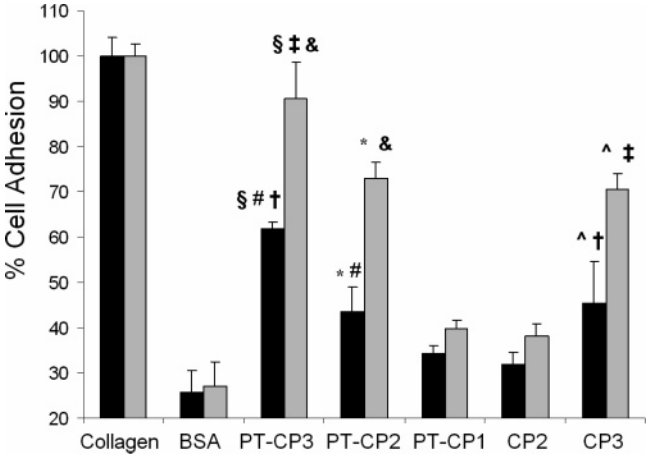

Figure 4. Adhesion of Hep3B (black) and L929 (gray) cells as a function of surface composition: calf-skin collagen (Collagen), 1% heat-denatured BSA (BSA), PT-CP3, PT-CP2, PT-CP1, CP2, and CP3. Cells in serum-free medium were allowed to adhere to a peptide- or protein-coated well plate for 1 h at 20 °C. Student's *t* test with $p < 0.05$: §,*, #, †, ^, &, and ‡ are significantly different from each other. Each histogram represents the mean ± SD with $n = 6$.

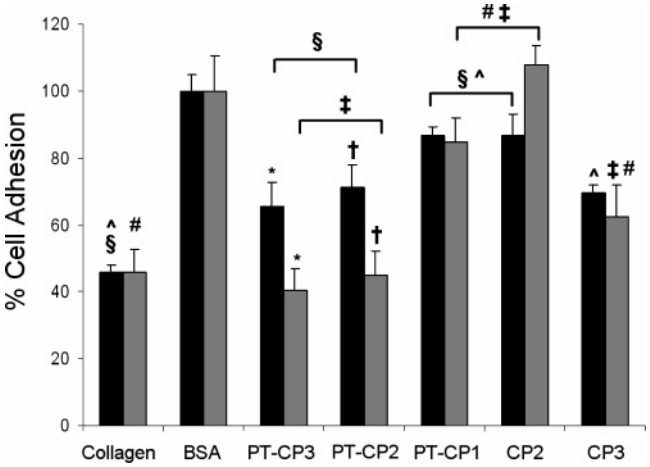

Figure 5. Competition inhibition of Hep3B (black) and L929 (gray) cell adhesion to the collagen-coated surface. Cells in serum-free medium were incubated with 50 μg/mL peptide or collagen for 30 min prior to seeding. The competitive adhesion was allowed to take place for 1 h at 20 °C. Cell adhesion in blank serum-free medium was used as a positive control. Student's *t* test with $p < 0.05$: §,*, #, †, ^, and ‡ are significantly different from each other. Each histogram represents the mean ± SD with $n = 3$.

lower T_m values (20 and 25 °C, respectively) and thus may undergo some degree of dissociation. Conversely, CP2 cannot assume a triple-helix structure. These conformation differences resulted in a considerable loss of recognition by both Hep3B and L929 cells. It is interesting to note that both PT-CP2 and CP3 promoted cell adhesion at a comparable level, probably because of their similar triple helicity. The result indicates that the activity of different collagen peptides supplemented with the same binding motif (GFOGER) may be similar if their triple helicity is comparable, highlighting the importance of triple-helical conformation in preserving the GFOGER cell binding site. The triple helix structure has been shown to be essential, if not crucial, for influencing cell adhesion, spreading, migration, matrix metalloproteinase binding, and human platelet adhesion and aggregation.[19,33,34,55] Similarly, the absence of the GFOGER hexapeptide in PT-CP1 caused a marked loss of activity and had an adverse effect on the level of cell adhesion, thus indicating the specific recognition of the GFOGER sequence by both cell types.

Although the presence of PT-CP3 promoted both Hep3B and L929 cell adhesion considerably, the two cell types displayed a significant difference in their recognition for the GFOGER sequence, as can be seen from the cell adhesion to PT-CP3, PT-CP2, and CP3. In all cases, the cell binding activity displayed by L929 cells was notably higher than that exhibited by Hep3B cells, suggesting that the collagen mimetics may have greater affinity for fibroblast receptors and that the mimicry of collagen cell adhesion by using a specific cell binding sequence may be different for various cell types. Although GFOGER has been shown as a major cell binding site in collagen,[21,33] it is not the only cell adhesion site within macromolecules, and it is not universally recognized by all cell integrin receptors. This could be one possible reason for the lack of recognition displayed by Hep3B cells. The integrins $\alpha_1\beta_1$, $\alpha_2\beta_1$, and $\alpha_{11}\beta_1$ have been shown to bind GFOGER and the GFOGER-like motifs found in collagen.[31,33,56,57] The difference in cell recognition is thus probably due to the difference in their expression of these specific integrins for GFOGER. Both hepatocytes and fibroblast cells have been shown to attach to natural collagen.[3,19,58] However, the repertoire of integrins expressed by hepatocytes is strikingly different from that of most other fibroblast cells. Platelets, epithelial cells, and fibroblasts have been shown to express high levels of $\alpha_2\beta_1$, which is the primary receptor for GFOGER and type I collagen.[21,33,57] In contrast, the collagen receptors $\alpha_2\beta_1$ usually expressed by epithelial cells are undetectable in normal adult hepatocytes.[59] Primary rat hepatocytes and fibroblasts both express the integrin $\alpha_1\beta_1$ that can function as a collagen receptor,[17] with the adult hepatocytes expressing only low levels of $\alpha_1\beta_1$ integrin, which is also true for Hep3B cells.[59] It is likely that the restricted expression of integrins by normal adult hepatocytes is an adaptation to their particular microenvironment.[59] In contrast to most epithelial cells, hepatocytes lack an organized basement membrane. Conversely, fibroblasts are the cells of connective tissues and are responsible for maintaining the structural integrity of the tissue by continuously secreting precursors of the ECM, especially collagen. Thus, the significant difference in the expression of integrins $\alpha_1\beta_1$ and $\alpha_2\beta_1$ by Hep3B and L929 cells may be a result of their adaptation to the different extracellular microenvironments and therefore result in the different cell binding activity of Hep3B and L929 cells on the GFOGER surfaces. A specific cell binding motif may not be recognized by a wide range of integrin receptors expressed on a specific cell type, and thus the use of a combination of cell binding sequences is necessary to better mimic ECM cell adhesion for optimized cell and tissue engineering. A combination of peptide models of collagen integrin-binding sequences and other ECM sequences has been studied previously and found to have potential to mimic the biological activities of an ECM.[60,61]

Competitive Inhibition of Hep3B and L929 Cell Adhesion to Collagen. The competitive inhibition assay is an indirect screening for the cell binding activity displayed by different cell types for the collagen or collagen peptides. The cells were preincubated with soluble collagen or collagen peptides prior to being seeded onto collagen-coated plates. Cell adhesion to the collagen surface is inhibited when the cell surface receptors, especially specific collagen receptors, are presaturated with the adhesive molecules prior to cell seeding. Adhesion of cells onto the collagen surface in blank serum-free medium was used as the 100% reference level.

It can be seen from Figure 5 that both cell types displayed specific interactions with the soluble collagen, and thus the cell adhesion to the collagen surface was significantly inhibited by

the presence of soluble collagen molecules in the competitive inhibition assay. The inhibition of adhesion of both cell types to the collagen surface by soluble collagen was comparable, indicating that both cells may recognize native collagen at a similar level and suggesting that GFOGER is not the only major cell adhesion sequence within the collagen macromolecules. In fact, both cell types may express similar integrins for other cell binding sequences of collagen, as demonstrated in the following cell adhesion assay.

The inhibitory activity of PT-CP2 and PT-CP3 was comparable to that of collagen for L929 cell adhesion. The GFOGER-containing triple-helical PT-CP2 and PT-CP3 effectively inhibited L929 cell binding to collagen. The inhibition was most probably due to the specific interactions between the GFOGER and the specific surface receptors, suggestive of the participation of specific collagen receptors in the adhesion process. The inhibition of Hep3B cell adhesion by the PT-assembled collagen peptides, however, was not comparable to the collagen. Hep3B cells displayed higher cell binding activity than L929 cells during the competitive inhibition, indicating the lack of specific interaction between the GFOGER sequences with the cell surface receptors. The result is in agreement with the cell adhesion assay, which showed that Hep3B and L929 cells may express integrins involved in the specific interaction with GFOGER, such as $\alpha_1\beta_1$ and $\alpha_2\beta_1$, at different levels. Removal of the GFOGER sequence or loss of the triple helical structure resulted in collagen peptides lacking the ability to inhibit the integrin-mediated cell adhesion process, as can be seen from the lower inhibitory activity displayed by PT-CP1 and CP2.

Cell Adhesion to Native and Denatured Collagen and PT-Assembled Collagen Peptides. Several cells have been shown to recognize native and denatured collagen.[3,62] Here, we studied the specific cell binding activity of Hep3B and L929 cells to native and denatured collagen and PT-assembled collagen peptides supplemented with GFOGER. The triple helical structure has been shown to be important for both Hep3B and L929 cell attachment to GFOGER through the cell adhesion assay using a series of PT-assembled collagen peptides of different triple helicities as a model for natural collagen. However, the recognition of the cells over a specific substrate, such as collagen or PT-CP3, when the substrate is heat-denatured is not fully known. This study was performed to further investigate the role of the triple-helical molecular architecture in the specific recognition of Hep3B and L929 cells over the GFOGER sequence and collagen. The denatured substrates were prepared by heating collagen and PT-assembled collagen peptide solutions at 70 °C for 3 h immediately before incubation in the microwell plate at 70 °C overnight.[3] Cell adhesion to the native collagen substrate was used as the 100% reference level.

The collagen triple helix appears to be an important recognition element for both Hep3B and L929 cells, as can be seen from the reduction of the cell adhesion to the denatured collagen substrate. The result is consistent with the fact that native collagen has a noticeably higher affinity for collagen-specific receptors than denatured collagen.[17,63] The cell adhesion of both cell types was reduced at a similar degree to ~55% (Figure 6), suggesting a similar recognition of both cells over the denatured collagen. The cell adhesion to denatured collagen, although lower, is still significant, indicating that the triple helix is important, but not crucial, for cell adhesion to collagen. This result suggests that both Hep3B and L929 cells express integrins that are involved in the adhesion to denatured collagen, such as $\alpha_5\beta_1$ and $\alpha_v\beta_3$,[17,62,64,65] but are not involved in adhesion to triple-helical GFOGER at a similar level. The sequences

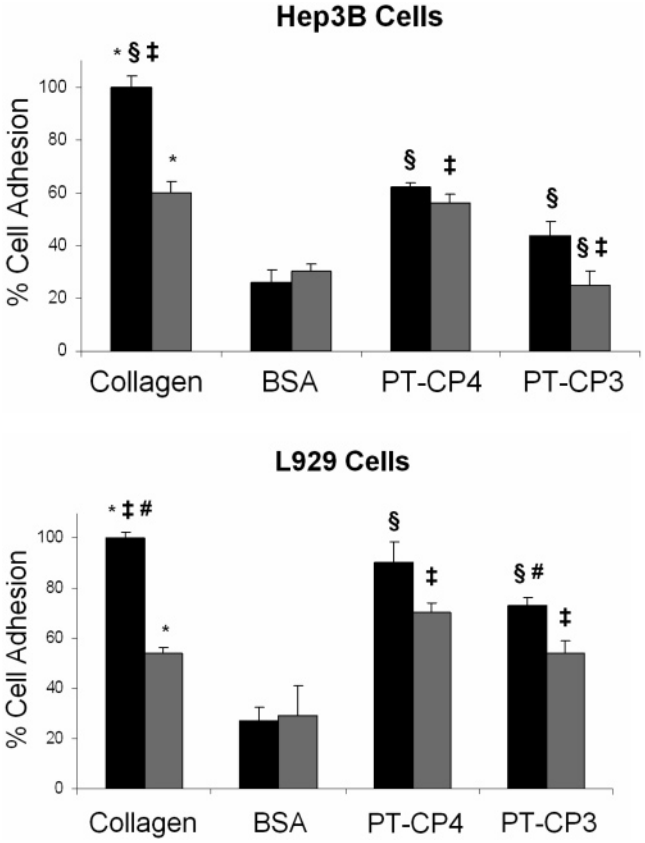

Figure 6. Adhesion of Hep3B (a) and L929 (b) cells as a function of surface composition coated at different temperatures overnight: 4 °C (black) and 65 °C (gray). Cells in serum-free medium were allowed to adhere to a peptide- or protein-coated well plate for 1 h. Student's *t* test with $p < 0.05$: §,*, #, and ‡ are significantly different from each other.

involved in cell adhesion to denatured collagen are probably DGEA[66] and RGD.[17,64] Conversely, the cell surface receptors that are responsible for adhesion to GFOGER, such as $\alpha_1\beta_1$, $\alpha_2\beta_1$, and $\alpha_{11}\beta_1$[31,33,56,57] were expressed by Hep3B and L929 cells at different levels.

While the adhesion of both Hep3B and L929 cells was reduced by approximately 50% on the denatured collagen, the cell binding activity to the denatured PT-assembled collagen peptides, especially PT-CP3, was almost preserved, which we attribute to the stabilizing effect of the PT in promoting the assembly of the short collagen peptides into the triple-helical conformation. In contrast, the cell adhesion to the non-triple-helical GFOGER (CP2) was significantly reduced (Figure 4). It has been demonstrated that the degree of conformational change of the PT-assembled collagen peptides is much smaller compared to that of the calf-skin collagen at elevated temperatures (Figure 2), probably because of the stabilizing effect of the template, which promotes interactions between the peptides and overcomes the unfavorable entropy. This result suggests that collagen peptides can be used as a stable triple-helical molecular architecture with a proper template assembly strategy to improve their cell recognition by supplementing them with a specific cell binding sequence. It is also interesting to note that the L929 cells displayed a higher binding activity than the Hep3B cells in adhering to the denatured PT-assembled collagen peptides, consistent with the result of the cell adhesion assay, suggesting that the expression of integrins for collagen GFOGER may be different by various cell types.

Cytoskeletal Organization and Focal Adhesion Immunofluorescence Staining for Hep3B and L929 Cells. Hep3B

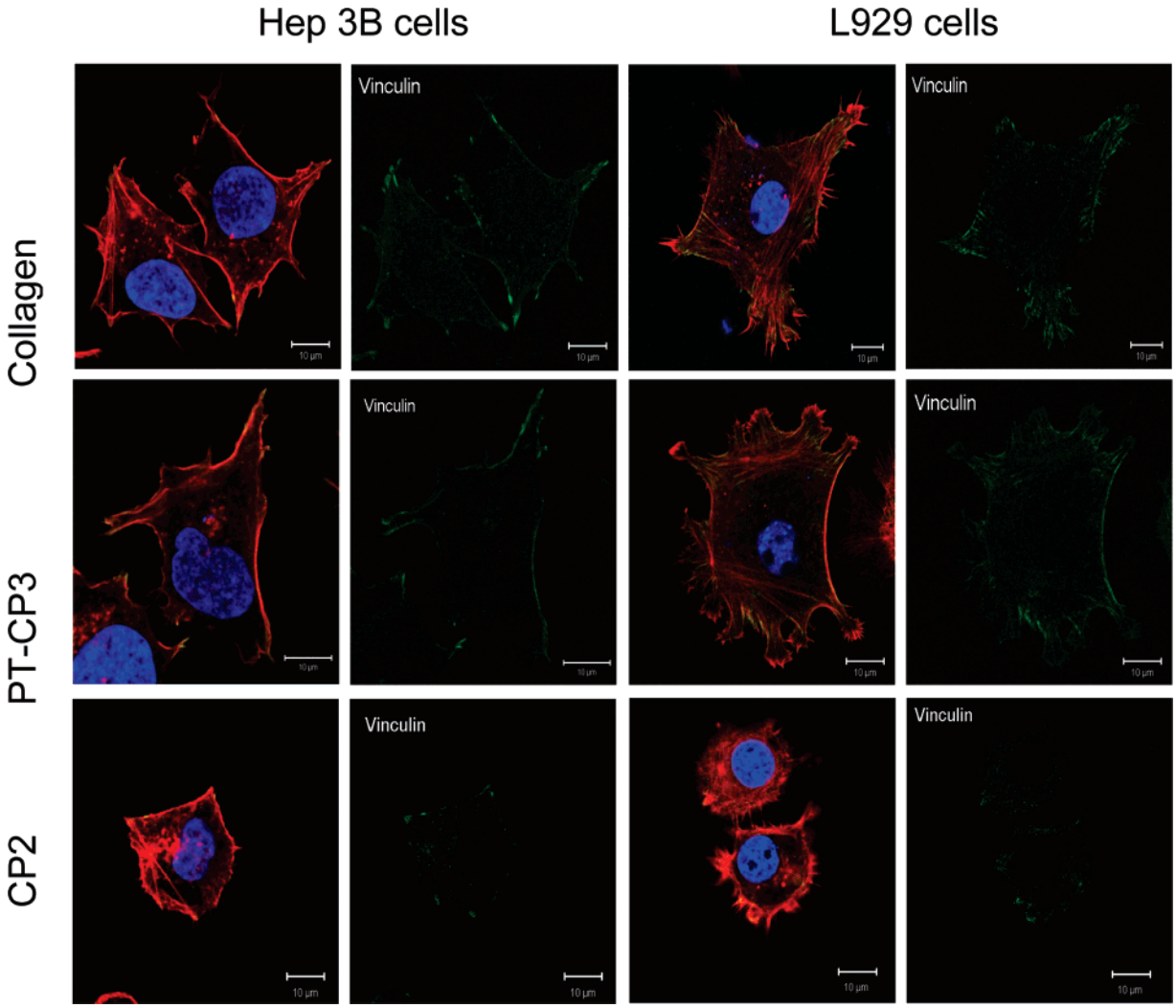

Figure 7. Cytoskeletal organization and focal adhesions of Hep3B and L929 cells as a function of substrates: collagen, PT-CP3, and CP2. Cells were fixed and stained for actin stress fibers (TRITC−phalloidin; red), nuclei (DAPI; blue), and vinculin (FITC−antivinculin; green) after 3 h of adhesion in serum-free medium and examined by confocal microscopy (60× magnification).

and L929 cells seeded on collagen, PT-CP3, and CP2 substrates were fixed and stained at 3 h for actin stress fibers (TRITC−phalloidin; red), nuclei (DAPI; blue), and vinculin (FITC−antivinculin; green), a major membrane−cytoskeletal protein present in focal adhesion plaques that is involved in the linkage of integrins to actin cytoskeleton,[67] to study the cytoskeletal organization and focal adhesion formation. The confocal images are presented in Figure 7.

It can be seen from the confocal images that both cell types displayed well-developed actin cytoskeletal structure and collagen-like adhesion profiles on the PT-CP3 surface. Both Hep3B and L929 cells exhibited distinct actin stress fibers when seeded on collagen and PT-CP3 surfaces. The assembled elongated actin filaments indicated the formation of strong actin cytoskeleton organization in both cell types. Conversely, the actin organization became less pronounced on the cells seeded on non-triple-helical GFOGER (CP2) surfaces. While both Hep3B and L929 cells spread and developed extensive actin stress fibers on collagen and PT-CP3 surfaces, most of them remained in spherical morphology after 1 and 3 h adhesions on CP2 and PT-CP1 (result not shown). Deletion of the GFOGER sequence or loss of the triple helical structure caused a substantial decrease in the cell spreading activities.

Focal adhesions are sites where integrin-mediated adhesion links to the actin cytoskeleton. It can be seen from the vinculin staining (Figure 7) that both cells formed strong focal adhesion contacts on the collagen surface. Most of the focal adhesions were found at both the cell periphery and the center, associated with the ends of stress fibers of the cells. Although the recognition of the GFOGER sequence by different cell types cannot be measured quantitatively by immunofluorescence staining, it can be seen qualitatively from the confocal images that L929 cells exhibited a higher concentration of vinculin and thus more focal contacts compared to Hep3B cells on the PT-CP3 surface, indicating a more firm adhesion and more rapid interaction between the cell surface receptors and the GFOGER sequence. The localization of vinculin on the periphery and center, with a sharp spike at the termination points and across the actin stress fibers, of both cell types seeded on PT-CP3 suggests that the collagen peptides promoted the integrin-mediated cell adhesion in a pattern similar to that observed on the collagen surface. Conversely, both Hep3B and L929 cells displayed very few focal adhesion points when seeded on the CP2 surface. Cells did not form strong focal contacts on non-triple-helical GFOGER, as the vinculin are observed at relatively low densities at the periphery of the cells. The focal adhesion position at the convergence of integrin adhesion, signaling, and the actin cytoskeleton generally involve integral membrane protein integrins, which bind to extracellular proteins via specific amino acid sequences, such as the RGD motif. Therefore, we

hypothesize that cell adhesion and spreading on collagen and PT-CP3 surfaces are unlike the interaction between cells and synthetic polymers, which merely depends on the nonspecific contact between the cell membrane proteins and the functional groups of polymers.[68,69] The extensive cell spreading could, in fact, be a result of the integrin-mediated cell adhesion process.[2,47] Cell focal adhesion is important in regulating cellular behavior, including adhesion, signaling, migration, proliferation, and differentiation. Different cell types may recognize a specific cell binding sequence at a different degree. Therefore, mimicry of an ECM microenvironment using a specific or combination of various cell binding sequences to target a particular cell type is important to optimize a specific cell and tissue engineering.

Conclusion

PT-CP3 was shown to promote both Hep3B and L929 cell adhesion considerably. Cell recognition of the collagen peptides supplemented with GFOGER appeared to be both conformation- and sequence-specific, the absence of which resulted in a marked loss of cell recognition. The result may have great impact for biological chemists in their biomolecular design: shorter, and hence less expensive, collagen peptides can be used as a stable triple-helical molecular architecture with a proper template assembly strategy to improve their cell recognition by supplementing them with a specific cell binding sequence. However, it was also shown in this study that different cell types may recognize the GFOGER sequence at different levels. Although the GFOGER sequence appears to be a general cell adhesion-promoting site, there are differences in the levels of cell binding activity based on the cell types. A specific cell binding motif may not fully mimic an ECM microenvironment, and the use of a combination of two or more cell binding sequences, such as RGD, DGEA, and GFOGER, is necessary for targeting a wide range of integrin receptors expressed on a specific cell type to better mimic ECM cell adhesion.

Acknowledgment. We acknowledge support of this work by the National University of Singapore under Grant Number R279000168112.

Supporting Information Available. CD parameters, Rpn values, HPLC chromatograms, and MALDI-TOF MS spectra of each peptide. This material is available free of charge via the Internet at http://pubs.acs.org.

References and Notes

(1) Ruoslahti, E.; Reed, J. C. *Cell* **1994**, *77*, 477−478.
(2) Hynes, R. O. *Cell* **1992**, *69*, 11−25.
(3) Rubin, K.; Höök, M.; Öbrink, B.; Timpl, R. *Cell* **1981**, *24*, 463−470.
(4) Gumbiner, B. M. *Cell* **1996**, *84*, 345−357.
(5) Guler, M. O.; Hsu, L.; Soukasene, S.; Harrington, D. A.; Hulvat, J. F.; Stupp, S. I. *Biomacromolecules* **2006**, *7*, 1855−1863.
(6) Massia, S. P.; Stark, J. *J. Biomed. Mater. Res.* **2001**, *56*, 390−399.
(7) Yang, X. B.; Bhatnagar, R. S.; Li, S.; Oreffo, R. O. C. *Tissue Eng.* **2004**, *10*, 1148−1159.
(8) Qian, J. J.; Bhatnagar, R. S. *J. Biomed. Mater. Res.* **1996**, *31*, 545−554.
(9) Hanks, T.; Atkinson, B. L. *Biomaterials* **2004**, *25*, 4831−4836.
(10) Thorwarth, M.; Schultze-Mosgau, S.; Wehrhan, F.; Kessler, P.; Srour, S.; Wiltfang, J. r.; Schlegel, K. A. *Biomaterials* **2005**, *26*, 5648−5657.
(11) Reyes, C. D.; García, A. J. *J. Biomed. Mater. Res.* **2003**, *65A*, 511−523.
(12) Reyes, C. D.; García, A. J. *J. Biomed. Mater. Res.* **2004**, *69A*, 591−600.
(13) Perris, R.; Syfrig, J.; Paulsson, M.; Bronner-Fraser, M. *J. Cell Sci.* **1993**, *106*, 1357−1368.
(14) Faassen, A. E.; Schrager, J. A.; Klein, D.; Oegema, T. R.; Couchman, J.; McCarthy, J. B. *J. Cell Biol.* **1992**, *116*, 521−531.
(15) Grzesiak, J. J.; Davis, G. E.; Kirchhofer, D.; Pierschbacher, M. D. *J. Cell Biol.* **1992**, *117*, 1109−1117.
(16) Scharffetter-Kochanek, K.; Klein, C. E.; Heinen, G.; Mauch, C.; Schaefer, T.; Adelmann-Grill, B. C.; Goerz, G.; Fusenig, N. E.; Krieg, T. M.; Plewig, G. *J. Invest. Dermatol.* **1992**, *98*, 3−11.
(17) Gullberg, D.; Gehlsen, K. R.; Turner, D. C.; Åhlén, K.; Zijenah, L. S.; Barnes, M. J.; Rubin, K. *EMBO J.* **1992**, *11*, 3865−3873.
(18) Staatz, W.; Fok, K.; Zutter, M.; Adams, S.; Rodriguez, B.; Santoro, S. *J. Biol. Chem.* **1991**, *266*, 7363−7367.
(19) Grab, B.; Miles, A. J.; Furcht, L. T.; Fields, G. B. *J. Biol. Chem.* **1996**, *271*, 12234−12240.
(20) Renner, C.; Saccà, B.; Moroder, L. *Biopolymers* **2004**, *76*, 34−47.
(21) Knight, C. G.; Morton, L. F.; Onley, D. J.; Peachey, A. R.; Messent, A. J.; Smethurst, P. A.; Tuckwell, D. S.; Farndale, R. W.; Barnes, M. J. *J. Biol. Chem.* **1998**, *273*, 33287−33294.
(22) Ruoslahti, E.; Pierschbacher, M. D. *Science* **1987**, *238*, 491−497.
(23) Massia; Hubbell *J. Cell Biol.* **1991**, *114*, 1089−1100.
(24) Boateng, S. Y.; Lateef, S. S.; Mosley, W.; Hartman, T. J.; Hanley, L.; Russell, B. *Am. J. Physiol.: Cell Physiol.* **2005**, *288*, 30−38.
(25) Massia, S.; Rao, S.; Hubbell, J. *J. Biol. Chem.* **1993**, *268*, 8053−8059.
(26) Graf, J.; Ogle, R. C.; Robey, F. A.; Sasaki, M.; Martin, G. R.; Yamada, Y.; Kleinman, H. K. *Biochemistry* **1987**, *26*, 6896−6900.
(27) Fields, G. B. *Connect. Tissue Res.* **1995**, *31*, 235−243.
(28) Kramer, R.; Marks, N. *J. Biol. Chem.* **1989**, *264*, 4684−4688.
(29) Camper, L.; Hellman, U.; Lundgren-Akerlund, E. *J. Biol. Chem.* **1998**, *273*, 20383−20389.
(30) Velling, T.; Kusche-Gullberg, M.; Sejersen, T.; Gullberg, D. *J. Biol. Chem.* **1999**, *274*, 25735−25742.
(31) Zhang, W.-M.; Käpylä, J.; Puranen, J. S.; Knight, C. G.; Tiger, C.-F.; Pentikäinen, O. T.; Johnson, M. S.; Farndale, R. W.; Heino, J.; Gullberg, D. *J. Biol. Chem.* **2003**, *278*, 7270−7277.
(32) Kühn, K.; Eble, J. *Trends Cell Biol.* **1994**, *4*, 231−270.
(33) Knight, C. G.; Morton, L. F.; Peachey, A. R.; Tuckwell, D. S.; Farndale, R. W.; Barnes, M. J. *J. Biol. Chem.* **2000**, *275*, 35−40.
(34) Miles, A. J.; Skubitz, A. P. N.; Furcht, L. T.; Fields, G. B. *J. Biol. Chem.* **1994**, *269*, 30939−30945.
(35) Vandenberg, P.; Kern, A.; Ries, A.; Luckenbill-Edds, L.; Mann, K.; Kühn, K. *J. Cell Biol.* **1991**, *113*, 1475−1483.
(36) Feng, Y.; Melacini, G.; Taulane, J. P.; Goodman, M. *Biopolymers* **1996**, *39*, 859−872.
(37) Kajiyama, K.; Tomiyama, T.; Uchiyama, S.; Kobayashi, Y. *Chem. Phys. Lett.* **1995**, *247*, 299−303.
(38) Yamazaki, S.; Sakamoto, M.; Suzuri, M.; Doi, M.; Nakazawac, T.; Kobayashi, T. *J. Chem. Soc., Perkin Trans.* **2001**, *1*, 1870−1875.
(39) Ottl, J.; Moroder, L. *J. Am. Chem. Soc.* **1999**, *121*, 653−661.
(40) Ottl, J.; Battistuta, R.; Pieper, M.; Tschesche, H.; Bode, W.; Kühn, K.; Moroder, L. *FEBS Lett.* **1996**, *398*, 31−36.
(41) Feng, Y.; Melacini, G.; Taulane, J. P.; Goodman, M. *J. Am. Chem. Soc.* **1996**, *118*, 10351−10358.
(42) Goodman, M.; Feng, Y.; Melacini, G.; Taulane, J. P. *J. Am. Chem. Soc.* **1996**, *118*, 5156−5157.
(43) Greiche, Y.; Heidemann, E. *Biopolymers* **1979**, *18*, 2359−2361.
(44) Thakur, S.; Vadolas, D.; Germann, H. P.; Heidemann, E. *Biopolymers* **1986**, *25*, 1081−1086.
(45) Roth, W.; Heidemann, E. *Biopolymers* **1980**, *19*, 1909−1917.
(46) Fields, C. G.; Lovdahl, C. M.; Miles, A. J.; Hageini, V. L. M.; Fields, G. B. *Biopolymers* **1993**, *33*, 1695−1707.
(47) Fields, C. G.; Mickelson, D. J.; Drake, S. L.; McCarthy, J. B.; Fields, G. B. *J. Biol. Chem.* **1993**, *268*, 14153−14160.
(48) Brown, F. R.; Corato, A. D.; Lorenzi, G. P.; Blout, E. R. *J. Mol. Biol.* **1972**, *63*, 85−99.
(49) Sakakibara, S.; Kishida, Y.; Okuyama, K.; Tanaka, N.; Ashida, T.; Kakudo, M. *J. Mol. Biol.* **1972**, *65*, 371−372.
(50) Kwak, J.; Capua, A. D.; Locardi, E.; Goodman, M. *J. Am. Chem. Soc.* **2002**, *124*, 14085−14091.
(51) Jefferson, E. A.; Locardi, E.; Goodman, M. *J. Am. Chem. Soc.* **1998**, *120*, 7420−7428.
(52) Bella, J.; Brodsky, B.; Berman, H. M. *Structure* **1995**, *3*, 893−906.
(53) Bella, J.; Eaton, M.; Brodsky, B.; Berman, H. M. *Science* **1994**, *266*, 75−81.
(54) Feng, Y.; Melacini, G.; Goodman, M. *Biochemistry* **1997**, *36*, 8716−8724.
(55) Fields, G. B. *J. Theor. Biol.* **1991**, *153*, 585−602.

(56) Xu, Y.; Gurusiddappa, S.; Rich, R. L.; Owens, R. T.; Keene, D. R.; Mayne, R.; Hook, A.; Hook, M. *J. Biol. Chem.* **2000**, *275*, 38981−38989.
(57) Siljander, P. R.-M.; Hamaia, S.; Peachey, A. R.; Slatter, D. A.; Smethurst, P. A.; Ouwehand, W. H.; Knight, C. G.; Farndale, R. W. *J. Biol. Chem.* **2004**, *279*, 47763−47772.
(58) Jokinen, J.; Dadu, E.; Nykvist, P.; Käpylä, J.; White, D. J.; Ivaska, J.; Vehviläinen, P.; Reunanen, H.; Larjava, H.; Häkkinen, L.; Heino, J. *J. Biol. Chem.* **2004**, *279*, 31956−31963.
(59) Nejjari, M.; Hafdi, Z.; Dumortier, J.; Bringuier, A.-F.; Feldmann, G.; Scoazec, J.-Y. *Int. J. Cancer* **1999**, *83*, 518−525.
(60) Malkar, N. B.; Lauer-Fields, J. L.; Juska, D.; Fields, G. B. *Biomacromolecules* **2003**, *4*, 518−528.
(61) Baronas-Lowell, D.; Lauer-Fields, J. L.; Fields, G. B. *J. Biol. Chem.* **2004**, *279*, 952−962.
(62) Tuckwell, D.; Ayad, S.; Grant, M.; Takigawa, M.; Humphries, M. *J. Cell Sci.* **1994**, *107*, 993−1005.
(63) Santoro, S. A. *Cell* **1986**, *46*, 913−920.
(64) Davis, G. E. *Biochem. Biophys. Res. Commun.* **1992**, *182*, 1025−1031.
(65) Pfaff, M.; Aumailley, M.; Specks, U.; Knolle, J.; Zerwes, H. G.; Timpl, R. *Exp. Cell Res.* **1993**, *206*, 167−176.
(66) Yamamoto, K.; Yamamoto, M. *Exp. Cell Res.* **1994**, *214*, 258−263.
(67) Ezzell, R. M.; Goldmann, W. H.; Wang, N.; Parasharama, N.; Ingber, D. E. *Exp. Cell Res.* **1997**, *231*, 14−26.
(68) Bačáková, L.; Mareš, V.; Bottone, M. G.; Pellicciari, C.; Lisá, V.; Švorčík, V. *J. Biomed. Mater. Res.* **2000**, *49*, 369−379.
(69) Bačáková, L.; Walachová, K.; Švorčík, V.; Hnatowicz, V. *Biomaterials* **2000**, *21*, 1173−1179.

BM700587J